Four-Channel All-Fiber Dispersion-Managed 2R Regenerator

Christos Kouloumentas, Lionel Provost, Francesca Parmigiani, Stamatios Tsolakidis, Periklis Petropoulos, Ioannis Tomkos, *Member, IEEE*, and David J. Richardson, *Member, IEEE*

***Abstract*—We experimentally investigate a dispersion-managed four-channel 2R regenerator that relies on self-phase modulation-induced spectral broadening and offset filtering at four shifted wavelengths. The device consists of several alternating sections of dispersion-compensating fibers and single-mode fibers. Due to this arrangement and the use of low duty-cycle return-to-zero pulses, nonlinear interchannel effects are sufficiently mitigated resulting in almost no additional degradation compared to the single-channel case.**

***Index Terms*—Dispersion management, multiwavelength regeneration, nonlinear fibers, self-phase modulation (SPM).**

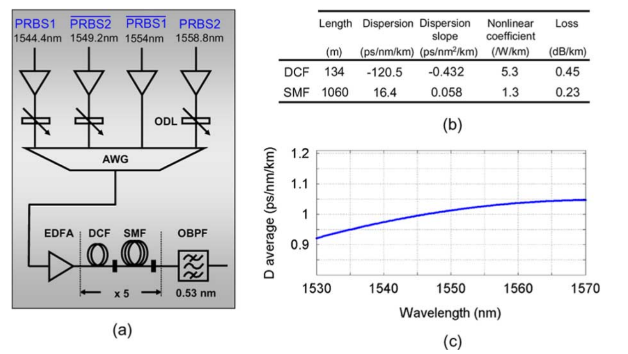

	Length (m)	Dispersion (ps/nm/km)	Dispersion slope (ps/nm²/km)	Nonlinear coefficient (/W/km)	Loss (dB/km)
DCF	134	-120.5	-0.432	5.3	0.45
SMF	1060	16.4	0.058	1.3	0.23

(b)

Fig. 1. (a) Experimental setup, (b) fibers' parameters, and (c) wavelength dependence of the average dispersion.

I. INTRODUCTION

MULTIWAVELENGTH regeneration is envisaged as a key functionality in future optical networks with potential to provide major technical and economical benefits. Efforts have been made over recent years to scale the all-optical fiber-based 2R regeneration techniques from a single- to a multichannel operation. Given that these techniques are based on strong nonlinear effects inside optical fibers, the success of the multiwavelength operation mainly relies on the mitigation of nonlinear interchannel effects, i.e., cross-phase modulation (XPM) and four-wave mixing. To date, only a few experimental attempts of simultaneous 2R regeneration have been described, relying either on soliton-like compression in a dispersion map [1] or self-phase modulation (SPM)-induced spectral broadening and offset filtering (also known as Mamyshev technique [2]), using a dispersion decreasing fiber [3] or bidirectional propagation in a polarization maintaining fiber [4]. Efficient multiwavelength operation of the Mamyshev regenerator with uni-directional data flow has been theoretically proposed by introducing suitable dispersion management [5]–[7]. In the present work, we report and further interpret the first experimental attempt with the latter scheme using four 600-GHz-spaced 10-Gb/s wavelength-division-multiplexing (WDM) channels within an all-fiberized dispersion-managed device [8].

The proposed regenerator deploys a fiber-based dispersion map that ensures high local and low average dispersion value along the device [see Fig. 1(a)]. In this way, the nonlinear interchannel effects are significantly weaker due to the fast walk-off time between pulses of adjacent channels, while the potential for SPM-induced spectral broadening is sufficiently retained. Originally, the idea of employing dispersion management to facilitate multichannel operation was introduced in [5], considering nonlinear fibers of high normal dispersion, e.g., dispersion-compensating fiber (DCF), separated by periodic group delay devices (PGDDs). PGDD reduce the bit-pattern dependence of the nonlinear crosstalk by allowing the pulses to uni-directionally walk-through each other. In [6], a more practical scheme was proposed by replacing the PGDD with single-mode fiber (SMF). Despite the modification in the pulse interaction process (in this case pulses of interfering channels walk back and forth relative to each other), multichannel regeneration can still be sustained provided that a strong dispersion map and a positive average dispersion are maintained [6], [7]. In fact, the dispersion map strength determines the relative strength of the useful SPM-induced phase shift with respect to the most destructive form of XPM-induced phase shift that originates from an incomplete passing through of pulses in different channels.

Herein, we describe the experimental proof-of-principle for the design proposed in [6], when four 600-GHz-spaced WDM channels at 10 Gb/s are considered. Preliminary simulations allow for envisaging the cascadeability of the regenerator [6].

Manuscript received December 12, 2007; revised March 5, 2008. This work was supported in part by the EU STREP Project TRIUMPH and the EU COST 291 action.

Ch. Kouloumentas, S. Tsolakidis, and I. Tomkos are with the Athens Information Technology Center (AIT), 19002 Peania, Greece (e-mail: ckou@ait.gr).

L. Provost, F. Parmigiani, P. Petropoulos, and D. J. Richardson are with the Optoelectronics Research Centre, University of Southampton, Southampton SO17 1BJ, U.K.

Color versions of one or more of the figures in this letter are available online at http://ieeexplore.ieee.org.

Digital Object Identifier 10.1109/LPT.2008.924896

II. EXPERIMENTAL SETUP—SIMULATION RESULTS

The experimental setup is shown in Fig. 1(a). Four WDM channels with the spectral allocation reported in Fig. 1(a) are amplitude modulated by four $2^{31}-1$ long pseudorandom bit sequences (PRBS) at 10 Gb/s. Channel power equalization is provided via optical preamplifiers, while optical delay lines (ODLs) adjust the initial delays between the channels. The channels are multiplexed by a 50-GHz bandwidth arrayed waveguide grating

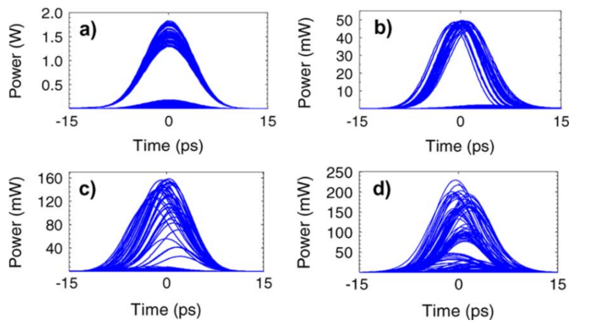

Fig. 2. Simulation results: (a) Degraded input signal. Worst channel output for: (b) the dispersion-managed regenerator, (c) a single-fiber regenerator with the same accumulated dispersion, and (d) a single-fiber regenerator exhibiting similar TFs as the implemented system.

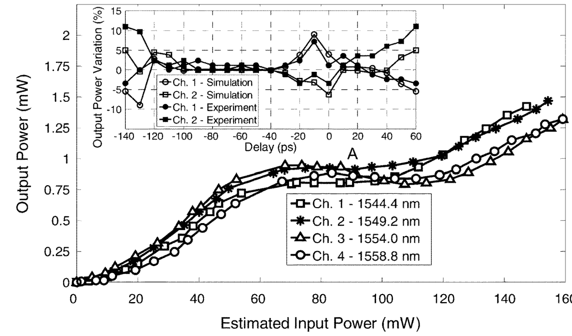

Fig. 3. Experimental TFs. Inset: Output power variation of channels 1 and 2 compared to the single-channel case, for different values of time delay between the two channels. Positive delay indicates precedence of channel 1.

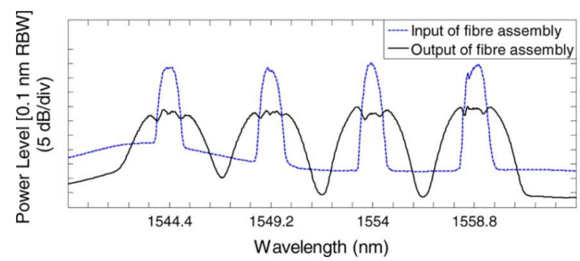

Fig. 4. Spectrum of the WDM signal (10-Gb/s PRBS in each channel) at the input and output of the dispersion-managed fiber assembly.

(AWG), and enter the regenerator. Characterization of pulses at the AWG's output, revealed a pulsewidth of 7.9, 8.1, 8.6, and 8.8 ps for channels 1–4, respectively, indicating a variable amount of chirp among the channels.

The regenerator encompasses a high-power amplifier, the assembled fiber section, and a tunable bandpass filter of 0.53-nm bandwidth, which acts as the output decision element. Optimization of the filter detuning resulted in an offset of -0.7 nm as compared to the carrier wavelength for all channels. The fiber assembly comprises five identical pairs of DCF and SMF pieces with the parameters given in Fig. 1(b). The DCF length was selected to exhibit a maximum differential group delay of $\sim$75 ps between two adjacent channels, and the SMF length was chosen to adjust the average dispersion at nearly $+1$ ps/nm/km, as shown in Fig. 1(c). The insertion loss of the 5970-m-long fiber assembly is $\sim$9 dB, mainly due to the splices between DCF and SMF ($\sim$1 dB/splice). Optimization of the splices would result in lower insertion loss, and thus better overall performance, similarly to what was predicted for the quasi-continuous filtering-based 2R regenerator [9].

A simulation study based on the setup parameters was conducted, considering four 10-Gb/s uncorrelated signals, deterministically degraded as shown in Fig. 2(a). The pulses of the four channels were assumed aligned at the fiber assembly input. In Fig. 2(b), the worst channel output is depicted. When the dispersion map was replaced by a 5970-m-long single fiber with the same nonlinearity as the DCF and dispersion equal to the average dispersion of the fiber assembly, the outputs were heavily distorted due to nonlinear crosstalk, as it is shown for the worst-channel output in Fig. 2(c). Heavy distortion is also observed in Fig. 2(d) in the case of a normal dispersion single-fiber regenerator, whose parameters (fiber with 800-m length, -3.5-ps/nm/km dispersion, -0.01-ps/nm^2/km dispersion slope, 10.5-W^{-1} $\cdot$ km^{-1} nonlinearity, 2-dB/km attenuation, and subsequent 0.53-nm filter at 0.8-nm offset) were chosen according to the design rules reported in [10], so that its input–output power transfer functions (TFs) closely resemble the TFs of the dispersion-managed regenerator. In all three cases, the input power was optimized. It is also noted that single-channel regeneration could be achieved in all cases. These results reveal the anticipated key-role of the dispersion management in the mitigation of the nonlinear crosstalk.

III. Experimental Results and Discussion

The power TFs were extracted for each channel separately, using mark pulses at a repetition of 5 GHz. The retrieved TFs, illustrated in Fig. 3, are in good agreement with supporting simulation results, which additionally indicate that the variation between the TFs is due to the characteristics of the input pulses, and not due to the wavelength dependence of the dispersion map. This is also understood by the low variation ($\pm$2%) of the average dispersion in the spectral range of interest [Fig. 1(c)]. A first investigation of the nonlinear crosstalk was conducted by studying the impact of the initial time delay τ between two adjacent channels at the input of the device. Channels 1 and 2 were considered using again sequences consisting of mark pulses at 5-GHz repetition rate. These sequences enable the consideration of the dominant pulse interactions in the 10-Gb/s system, since the dispersion map allows in such a system every pulse to mainly interact with only a single pulse of the adjacent channels. The input power per channel was set to $\sim$90 mW (point A in Fig. 3), and the output power as a function of τ was monitored. The power variations relative to the single-channel case for each channel are summarized in the inset of Fig. 3. Maximum variation reaching 11% is observed for $\tau \sim 60$ ps, with positive values denoting precedence of channel 1. A second point of high variation lies at slightly negative values of τ. Both results were qualitatively confirmed by simulations, as shown.

The regenerator performance was investigated by bit-error-rate (BER) measurements for all channels in the presence and absence of interfering channels using 10-Gb/s PRBS signals. Each channel operated at 90 mW, and the results reported hereafter refer to what we believe to be a less favorable case for multichannel operation as shown in Fig. 3, i.e., $+60$-ps delay between adjacent channels. Moreover, it is noted that no degradation in the quality of the output signals was observed

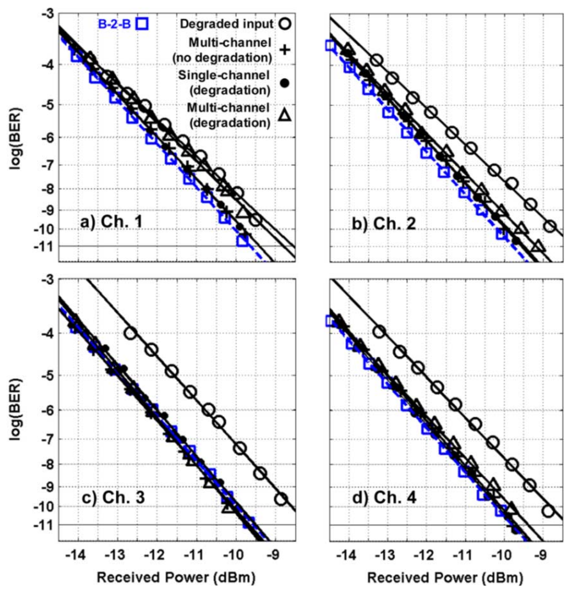

Fig. 5. Measured BER performance of channels in single- and multichannel operation: (a) Channel 1, (b) Channel 2, (c) Channel 3, and (d) Channel 4.

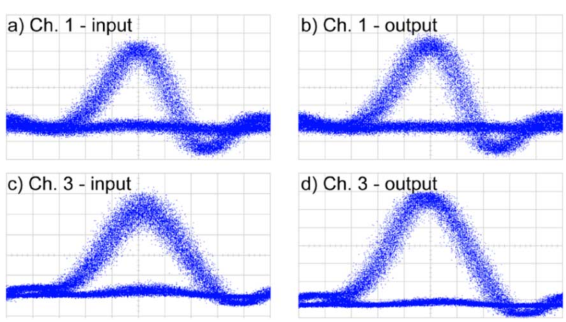

Fig. 6. Eye diagrams in four-channel operation. Channel 1: (a) input and (b) output of the regenerator. Channel 3: (c) input and (d) output of the regenerator.

when "random" relative delays were applied during our measurements. In Fig. 4, the spectrum of the WDM signal at the input and output of the fiber assembly is shown, indicating a sufficient SPM-induced broadening.

In single-channel operation with undegraded input, the absence of any detectable power penalty was noted compared to the back-to-back case (results not shown), indicating that the regenerator itself does not introduce additional penalty. Similar results were obtained in four-channel operation and are represented with crosses in Fig. 5, denoting the limited presence of interchannel crosstalk. When the input signal was artificially degraded by using a nonoptimum bias-voltage for the modulators, in single-channel operation, the noise could be partially suppressed for all channels, as it is illustrated with solid circles in Fig. 5. However, a performance variation can be recognized by the different amount of degradation applied on each channel, with channels 1 and 3 being the worst- and best-performing channels, respectively. The variation can be mainly related to the different extinction ratios of the TFs, seen in Fig. 3, and the favored distribution of the amplified spontaneous emission noise of the optical amplifier towards shorter wavelengths (see Fig. 4).

In four-channel operation, the regenerator could suppress the noise for channels 2, 3, and 4, as shown with triangles in Fig. 5, with the lower power penalty improvement being ~0.8 dB for channel 2 at BER $= 10^{-9}$. Eye diagrams of channels 1 and 3 at the input and output are depicted in Fig. 6. Even for the worst-performing channel 1, a limited degree of noise suppression in the space level is apparent. Although the performance variation among channels is slightly enhanced, it is noted that at the reference BER of 10^{-9}, the power penalty of the four-channel compared to the single-channel operation is lower than 0.5 dB for all channels, revealing sufficient mitigation of crosstalk and that single- and four-channel performances follow similar trends for each one of the channels.

It is noted that the pulses' low duty cycle (~8.3%) is among the main reasons for the achieved performance at 10 Gb/s. However, it is anticipated through our simulations that a data rate upgrade to 40 Gb/s (duty-cycle increase to ~33%), will allow the operation to be sustained at the expense of a higher input power, since the additional interchannel interaction (pulse collisions) will be counter-balanced by a higher pulse-averaging effect [6].

IV. Conclusion

Proof-of-principle operation of a dispersion-managed regenerator for simultaneous processing of four WDM channels at 10 Gb/s is presented. The scheme relies on alternating sections of DCF and SMF to mitigate the nonlinear interchannel effects. Despite a small residual crosstalk, the crosstalk mitigation achieves error-free operation for all channels, and regeneration with power penalty improvement up to 1.5 dB for degraded input signals. It is believed that 40-Gb/s operation is feasible at the expense of higher power requirements and only some slight performance degradation.

References

[1] T. Ohara, H. Takara, A. Hirano, K. Mori, and S. Kawanishi, "40-Gb/s × 4-channel all-optical multichannel limiter utilizing spectrally filtered optical solitons," *IEEE Photon. Technol. Lett.*, vol. 15, no. 5, pp. 763–765, May 2003.

[2] P. V. Mamyshev, "All-optical data regeneration based on self-phase modulation effect," in *Proc. ECOC 1998*, Sep. 1998, pp. 475–476.

[3] D. V. Kuksenkov, S. Li, M. Sauer, and D. A. Nolan, "Nonlinear fibre devices operating on multiple WDM channels," in *Proc. ECOC 2005*, Glasgow, U.K., Sep. 2005, vol. 1, pp. 51–54, Paper Mo.3.5.1.

[4] L. Provost *et al.*, "Simultaneous all-optical 2R regeneration of 4 × 10 Gbit/s wavelength division multiplexed channels," in *Proc. ECOC 2007*, Berlin, Germany, Sep. 2007, Paper Di 4.5.1.

[5] M. Vasilyev and T. I. Lakoba, "All-optical multichannel 2R regeneration in a fibre-based device," *Opt. Lett.*, vol. 30, no. 12, pp. 1458–1460, Jun. 2005.

[6] I. Tomkos, C. Kouloumentas, and S. Tsolakidis, "Performance studies of multi-wavelength all-optical 2R regeneration subsystems based on highly nonlinear fibres," in *Proc. ICTON 2007*, Rome, Italy, Jul. 2007, vol. 1, pp. 132–135, Paper Tu.C1.1.

[7] T. L. Lakoba and M. Vasilyev, "A new robust regime for a dispersion-managed multichannel 2R regenerator," *Opt. Express*, vol. 15, pp. 10061–10074, Jul. 2007.

[8] L. Provost *et al.*, "Experimental investigation of a dispersion-managed multi-channel 2R optical regenerator," in *Proc. OFC 2008*, San Diego, CA, Feb. 2008, Paper OThJ3.

[9] B. Cuenot and A. D. Ellis, "WDM signal regeneration using a single all-optical device," *Opt. Express*, vol. 15, pp. 11492–11499, Sep. 2007.

[10] L. Provost, C. Finot, K. Mukasa, P. Petropoulos, and D. J. Richardson, "Design scaling rules for 2R-optical self-phase modulation-based regenerators," *Opt. Express*, vol. 15, no. 8, pp. 5100–5112, 2007.